International Journal of GEOMATE, May, 2026 Vol.30, Issue 141, pp. 121-128
ISSN: 2186-2982 (P), 2186-2990 (O), Japan, DOI: https://doi.org/10.21660/2026.141.g15236
Geotechnique, Construction Materials and Environment

IMAGE-BASED ESTIMATION OF SOIL PARTICLE SIZE AS A SUPPLEMENT TO SIEVE ANALYSIS

*Jose Manuel U. Subido[1], Erica Elice Saloma Uy[2] and Joenel Gales Galupino[3]

[1,2,3]Department of Civil Engineering, De La Salle University, Philippines

*Corresponding Author, Received: 28 May 2025, Revised: 22 Dec. 2025, Accepted: 28 Dec. 2025

ABSTRACT: Particle size distribution is an important parameter influencing soil behavior. This parameter is identified using a combination of tests such as the sieve and hydrometer analyses to identify the potential characteristics and behavior of a soil sample. This study investigates the use of image processing techniques as a supplementary tool to traditional methods, enabling the rapid and detailed generation of particle size distribution curves. Twenty different soil samples were collected and prepared for imaging following controlled conditions. Only particles retained up to a No. 40 (0.420 mm) sieve were considered in the study. Camera and measurement calibrations, thresholding, and edge detection were performed to extract particle dimensions. Particle boundaries were identified to estimate particle sizes using pixel to real-world measurement conversions. At least one of the dimensions taken from the particle is expected to be of greater value than a reference value from the sieve openings where it was retained to ensure that there is an accurate result in the particle size estimation. The test results showed a close correlation between the estimated particle size distribution and sieve analysis using the maximum Feret diameter. However, there is an observable decline in accuracy when the particle size decreases. The proposed method has potential to capture particle size and be further studied for use in the development of particle size distribution curves, confirming its viability as a supplementary technique.

Keywords: Particle Size Distribution, Image Processing, Camera Calibration, Sieve Analysis, Feret Diameter

1. INTRODUCTION

Soil is a heterogeneous material composed of minerals, organic matter, and void spaces, serving as the fundamental support for all engineered structures [1]. In geotechnical engineering, the assessment of soil physical properties is essential for the safe and efficient design of foundations, embankments, and other infrastructures. Among these properties, grain size distribution significantly influences the strength, permeability, and compressibility of soil [2,3]. The conventional laboratory methods used to determine particle size distribution are the sieve and hydrometer analyses [4,5]. However, these methods require extensive sample preparation and are limited in capturing finer details such as particle shape [6]. While standardized laboratory testing remains the cornerstone of accurate geotechnical characterization, there is growing value in integrating supplementary methods that can offer preliminary insights early in the assessment process. One key technique being explored is through imaging techniques.

Image-based techniques have been extensively studied across various disciplines of engineering due to their versatility, efficiency, and non-contact nature. Image processing procedures and classification have also been incorporated in land use classification, field assessment of dams, strength evaluation of steel and concrete beams [7-10]. The rapidly growing range of applications highlights the adaptability of image-based techniques in addressing complex engineering problems that traditionally relied on labor-intensive and subjective inspection methods. This also aligns with the rapid advancements in imaging techniques, bridging gaps between traditionally distinct engineering fields to maximize the efficiency, accuracy, and objectivity of assessment methods. In this context, using image-based techniques to estimate soil particle size is another way of introducing a supplementary, quantitative approach that enhances conventional laboratory testing while minimizing subjectivity and procedural limitations.

Recent advancements have explored how image processing can be a supplementary technique for estimating particle size distribution. While a standard sieve analysis makes use of mass relations, image-based techniques use individual grain geometry to compute the percent finer needed to construct the particle-size distribution curve [11-13]. These non-contact techniques have shown potential in advancing the body of knowledge on soil characterization using images.

Analysis of particle dimensions is necessary in understanding soil behavior, as particle size influences key geotechnical parameters such as permeability, compaction, and shear strength. As such, various techniques have been explored to expand conventional particle size characterization methods beyond traditional laboratory testing, particularly through the integration of image-based and automated approaches that enable particle-level analysis. Recent studies have investigated potential use of this technique for individual particle assessments. In these studies, it was observed that soil

particles are heterogeneous in terms of shape, as shown in Figure 1. Since particles cannot be singularly classified based on the shapes shown, image processing can help establish measurements for particles that are irregularly shaped.

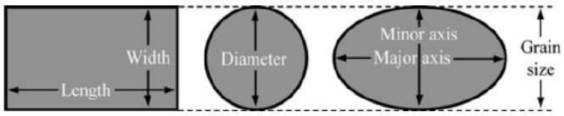

Fig. 1 Schematic Representation of Grain Size for Varying Particle Shapes [14]

Studies have integrated different preprocessing techniques which can improve the focus of the image towards the soil particles within the images used for particle size analysis [15,16]. Moreover, these studies also considered the use of different cameras with different capacities. However, these studies were limited to certain setups and the identification of a laboratory setup for image-based analysis of particle size [11-13]. Moreover, a common limitation within these studies is the lack of proper calibration procedures that can ensure accurate transformation of pixel-based measurements into real-world dimensions [11-16].

Calibration processes are performed to ensure that images acquired were without distortion and with proper scaling of measurements from pixel to real-world dimensions. Proper calibration corrects image distortion and ensures reliable scaling, as shown in Figure 2, where camera intrinsic and extrinsic parameters define the transformation from world coordinates to 2D image space [17,18]. Intrinsic parameters are used to transform points in the camera coordinate system to projection homogeneous coordinates. Conversely, the extrinsic parameters transform the points in the global world coordinate system of the camera coordinate system [17]. These parameters establish the accuracy and reliability of geometric transformations, thereby minimizing measurement errors of image-based analysis for real-world measurements.

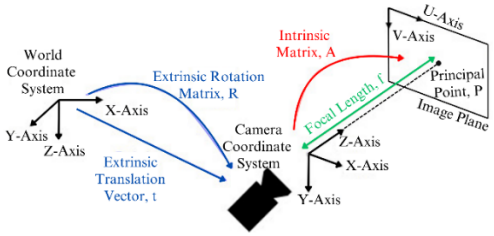

Fig. 2 Transformation of 3D to 2D system by images [17]

Despite the growing body of research on image-based soil particle size estimation, a key research gap remains in the lack of systematic validation of calibrated, particle-level image measurements against standard sieve analysis results. Many previous studies have employed simplified scaling assumptions or limited calibration procedures, thereby restricting the reliability and reproducibility of their findings [11-16]. In this study, samples with known particle size measurements were used to acquire soil images. The particle size measurements for individual particles were measured following a standard calibration procedure. Two dimensions were measured for each particle based on the bounding rectangle that was measured in the software. These dimensions were converted to real-world measurements and compared to sieve openings to identify if the estimated particle size matches the results of a sieve analysis. The soil images were subjected to image processing techniques such as thresholding and masking for feature extraction by converting raw soil images into analyzable data representations that highlight soil texture and composition after the calibration procedure was conducted. Unlike previous studies that focus on image processing performance, this study prioritizes calibration accuracy and direct experimental comparison with established laboratory methods, ensuring that the proposed image-based analysis as a validated supplementary tool.

The following sections discuss the significance of the study, the methodology employed, the results, discussion, and validation of the technique, and a summary of all the key findings and future research work aligned with the conclusion of the study.

2. RESEARCH SIGNIFICANCE

Particle size distribution is an important indicator that directly influences strength, compressibility, permeability, and overall performance of soil in geotechnical applications. The study highlights a significant advancement in soil particle size assessment by integrating image processing techniques as a supplementary tool to traditional methods. Unlike traditional sieve analysis, the proposed technique allows particle-level geometric evaluation, providing more detailed analysis on particle size characteristics.

By providing a faster and detailed estimation of particle size distribution, this approach enhances the efficiency of geotechnical investigations while maintaining alignment with standard practices. Furthermore, the integration of calibrated image analysis can support preliminary site assessments and improve decision-making in construction planning and geotechnical risk management by enabling faster assessment cycles and improved interpretation of soil behavior.

3. METHODOLOGY

The methodology is composed of five phases: sample preparation, setup preparation and calibration, image acquisition, image processing, and image

analysis. These phases collectively establish a procedure that ensures images were properly calibrated before it is processed and analyzed for particle-level size measurement with a comparison being made to conventional sieve analysis results.

3.1 Sample Preparation

A soil sample obtained from the City of Santa Rosa, Laguna, was subjected to ASTM-standard laboratory tests to establish its soil classification. The soil was classified as clayey sand (SC). The sample was oven-dried and clustered into particle size groups according to sieve sizes. A total mass of 500 grams was processed, but the analysis was limited to particles retained on the No. 40 sieve, thereby confining the evaluation of the proposed technique to coarse-grained soil particles. The particles were grouped based on the sieves where they were retained. The particle groups used in the study are shown in Table 1.

Table 1 Particle Clusters (PC) for Particle Size Analysis

PC (Sieve No.)	Particle Size Bounds (mm)
No. 4	> 4.750
No. 8	2.360 – 4.750
No. 10	2.000 – 2.360
No. 16	1.180 – 2.000
No. 30	0.600 – 1.180
No. 40	0.425 – 0.600

3.2 Setup Preparation and Calibration

A mirrorless camera was used to estimate the particle size of the sample. In this study, calibration was performed through a 2-dimensional calibration for distortion, and a measurement calibration using NI LabVIEW 2020. The distance of the camera from the soil sample surface and lighting conditions was determined through the 2D calibration [18]. A calibration grid, as shown in Figure 3, was used to convert the projected three-dimensional world points captured by an image to two-dimensional sensor coordinates. The grid is composed of dots with a radius of 2 mm and center-to-center distances of 1 cm. Ten images of the grid were acquired, at varying angles. In each trial of acquiring images of the grid, the set of images were collectively used to perform camera calibration [19]. However, if the calibration grid is not completely seen by the camera's field of view, the distance of the camera from the surface was adjusted accordingly. The grid images were only accepted if a large portion of the dots were identified by the program, which can be signified by having a distortion of less than 1% [20]. Once all images had a resulting distortion less than the threshold, the recorded intrinsic and extrinsic parameters were recorded. It was identified that the camera should be positioned 30 cm away from the sample to meet the threshold values. Shown in Figure 3 is the sample image of the grid after calibration. Each image was captured with a resolution of 2784x1856 pixels.

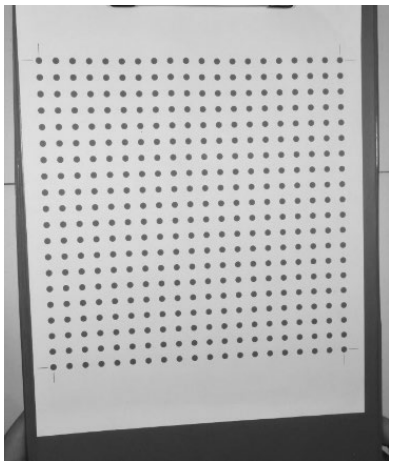

Fig. 3 Grayscale Calibrated Image of Grid

The next phase involved converting pixel data into real-world measurements using sieves and a ruler as reference objects, due to their known dimensions. A measurement calibration program was developed to determine x- and y-axis scaling factors, which convert pixel values into actual sizes [14,15]. These factors were validated by comparing program-measured values with known dimensions of sieve openings and ruler markings. The measured x and y-values in pixel measure were plotted against the actual values, as shown in Figure 4. From there, the slope of the best-fit line, where the y-intercept was set to 0, was identified. The slopes serve as the multiplying factor to convert real-world measurements to the pixel coordinate measurements. To convert vice-versa, the reciprocal of the slopes was taken and multiplied to the pixel measurements to establish the estimated real-world measurements from the image data. The factors for the x-direction and y-direction are 0.1232 mm/pixel and 0.1269 mm/pixel, respectively.

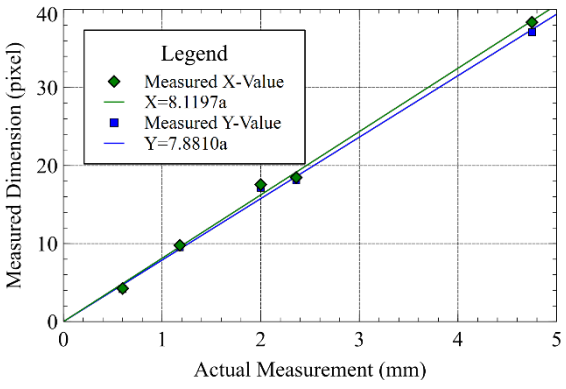

Fig. 4 Calibration Plot for Dimension Measurements

After calibration procedures were performed, the lighting conditions used in the study follows the schematic diagram of the image acquisition setup shown in Figure 5. The position of the camera was determined through calibration of parameters that can be identified from the camera's field of view [16-20].

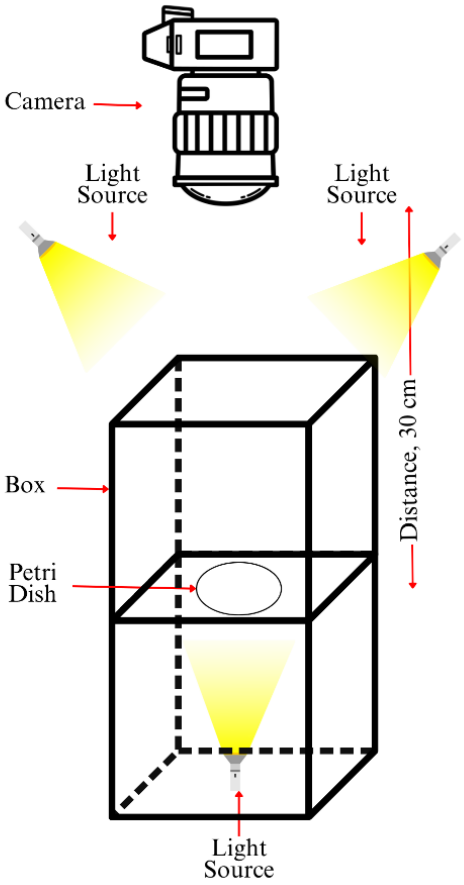

Fig. 5 Schematic Diagram of Image Acquisition Setup

3.3 Image Acquisition

The camera was configured with an aperture of f/16, a shutter speed of 1/80 second, ISO 1600, and no flash. Once the samples were separated into groups, each cluster was placed on the petri dish in such a way that majority of the particles were loosely positioned so that the individual particle measurements were evaluated by the proposed program. It is important to note that the arrangement of soil was altered in a way that there are extractable parameters for each model developed. To prevent reflection of light from affecting the particle size recorded, a thick piece of paper was used below the petri dish. Images were taken until 60 individual particles for each cluster group can be extracted using the particle size analysis program. Figure 6 presents the sample configuration for the particles within the petri dish, showing non-overlapping and overlapping particles.

Fig. 6 Raw Image of Particles Retained in No. 10 Sieve

3.4 Image Processing

The acquired images were processed for particle analysis using NI LabVIEW 2020. Each acquired image underwent image processing to reduce noise and ensure accurate extraction of particle characteristics. The region of interest (ROI) was isolated using a combination of masking and thresholding techniques. A circular mask was used to create a focus on the petri dish, with the center set using pixel data references and the edge was based on the real-world diameter of the petri dish. Thresholding was then applied to isolate soil particles from the background. The optimal threshold values were determined through an analysis of the gray level histogram, revealing that gray levels below 120 reflect the particle pixels. Shown in Figure 7 are the applied masking and thresholding into a sample image.

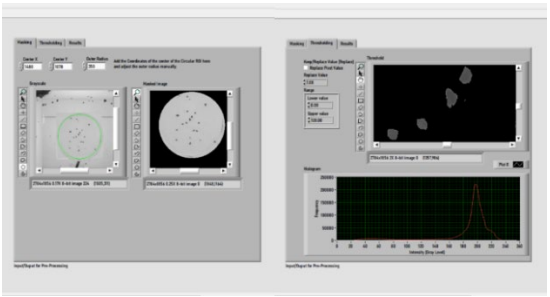

Fig. 7 ROI Extraction by Masking and Thresholding

The data gathered from images for particle size estimation focused only on particles that were loosely placed in the petri dish. In the analysis of particle size, the area was defined as the total number of pixels that were bound by the edge of the particle being analyzed. This serves as the frequency for a certain particle. Both dimensions from its bounding rectangle were considered as its particle size following the same convention as the sieve sizes. The larger dimension yielded the maximum particle size by image analysis, whereas the smaller dimension yielded the minimum particle size by image analysis. These values serve as the maximum and minimum Feret diameters recorded

in the program developed. For each particle, these parameters were extracted from LabVIEW using the IMAQ Particle Analysis VI. An example of feature extraction for the particle size estimation is shown in Figure 8.

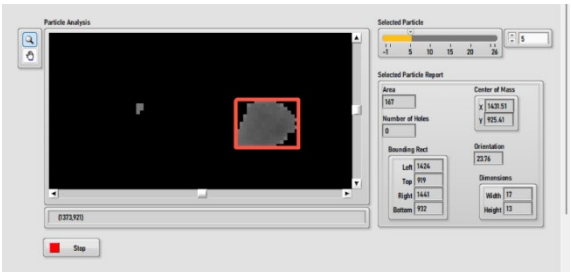

Fig. 8 Particle Size Analysis using NI LabVIEW 2020

3.5 Image Analysis

For each particle analyzed, the recorded dimensions were converted into real-world measurements and cross-validated with the group of soil particles to identify if the particle is retained on the sieve for that specific particle group. The particle size and area in real-world measurements are computed using the following equations:

$$PS_i = Max(W_i/x_{SF}, H_i/y_{SF}) \quad (1)$$

$$PS_i = Min(W_i/x_{SF}, H_i/y_{SF}) \quad (2)$$

$$A_i = A_{p,i} \times x_{SF} \times y_{SF} \quad (3)$$

where PS_i = particle size of particle i (mm); A_i = area of particle i (mm^2); W_i and H_i = width and height of particle i (pixel), $A_{p,i}$ = area of particle i (pixel); x_{SF} and y_{SF} = scaling factors for x- and y-axis (mm/pixel).

4. RESULTS AND DISCUSSION

The particle size was estimated based on the recorded dimensions of the bounding rectangle for each particle. The validation of values taken from the individual particle size characteristics was conducted by comparing the measured dimensions with the size of the sieves where the particles were retained. Only individual particles were considered in the study, with sample processed images shown in Figure 9. The individual particles are enclosed within bounding rectangles generated using the particle analysis feature of NI LabVIEW, where the corresponding length and width of each rectangle are measured in pixel units. When two or more particles overlap, this causes errors in how the rectangle is drawn over the packed particles. The measurements produced by the program correspond to packed particles, resulting in combined dimensions that do not accurately represent the true size of each individual particle. Including these particle measurements would introduce errors since these measurements are larger than the measurement intervals for each particle group considered. Instances of packed particles are shown in Figures 10 and 11.

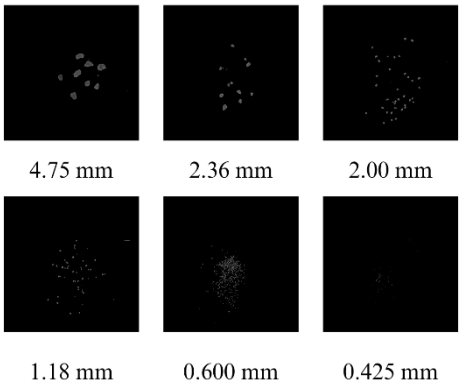

Fig. 9 Processed Images for Each Particle Size Group

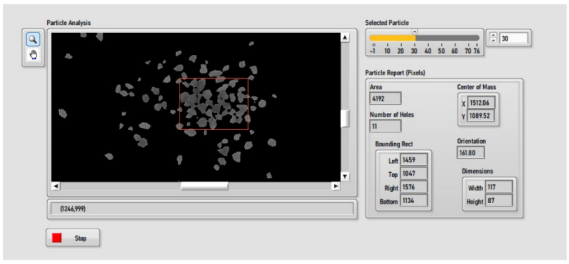

Fig. 10 Excluded Packed Particles from Particles Retained in No. 10 Sieve (2.000 mm – 2.360 mm)

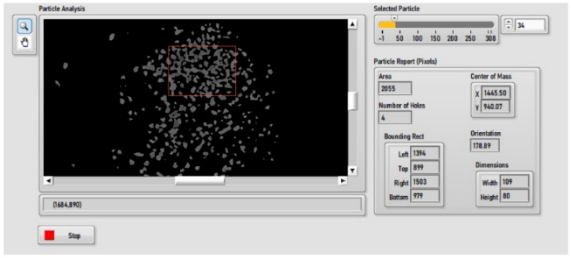

Fig. 11 Excluded Packed Particles from Particles Retained in No. 16 Sieve (1.180 mm – 2.000 mm)

To validate the accuracy of the estimation of particle size, two parameters were considered. Since particles were grouped based on the particle retained metric, each particle had to fall within the specified size intervals listed in Table 1. The first parameter involved calculating the cumulative area of particles that fell within these intervals and comparing it to the total area of all detected particles. The second parameter is taken by identifying the cumulative number of particles within the same intervals and comparing it to the total particle count. For both methods, the ratio of valid particles (by area or by count) to the overall total was used to determine the percentage accuracy of the program. Table 2 presents

the results based on the maximum Feret diameter of the particle (larger dimension of the particle's bounding rectangle) while Table 3 provides the results based on the minimum Feret diameter of the particle (smaller dimension of the particle's bounding rectangle). For both tables, the range of estimated particle sizes was also provided.

Table 2 Validation Metrics for Particle Size Estimation considering Maximum Feret Diameter

PC	%Accuracy by Area	%Accuracy by # of Particles	Range (mm)
No. 4	99.24%	98.33%	4.69 – 10.28
No. 8	85.14%	88.33%	2.03 – 5.42
No. 10	71.07%	71.67%	1.90 – 2.79
No. 16	95.68%	93.33%	1.11 – 2.03
No. 30	77.55%	85.00%	0.49 – 1.52
No. 40	69.58%	66.67%	0.25 – 0.63
Overall	94.53%	83.89%	0.25 – 10.28

Table 3 Validation Metrics for Particle Size Estimation considering Minimum Feret Diameter

PC	%Accuracy by Area	%Accuracy by # of Particles	Range (mm)
No. 4	96.02%	93.33%	4.44 – 8.13
No. 8	91.26%	86.67%	1.97 – 4.80
No. 10	29.88%	35.00%	1.48 – 2.41
No. 16	80.14%	68.33%	0.86 – 1.90
No. 30	85.99%	71.67%	0.37 – 1.11
No. 40	21.52%	16.67%	0.13 – 0.62
Overall	88.95%	61.94%	0.13 – 8.13

The results from Tables 2 and 3 highlighted that a difference exists in the accuracy of estimating particle size based on which dimension is used. When using the minimum dimension, accuracy by area and number of particles significantly decreased for particles retained on the No. 10 and No. 40 sieves. However, it is worth noting that for the particle group retained on the No. 30 sieve, the accuracy by area increased despite the decrease in the number of particles that were correctly classified. This observation was attributed to the larger area that each particle had for those that satisfy the criteria under consideration of minimum dimension compared to the maximum dimension. Nonetheless, the low accuracy in consideration of particle count highlights the tool's poor performance in estimating particle size using the minimum dimension.

The overall range of values indicated that the minimum particle size estimated by the developed program is 0.13 mm, which is also equivalent to the measure of 1 pixel along either the x- or y-axis, as taken from the measurement calibration. While this indicates that estimation is possible up to this degree, it is observed that the estimation accuracy becomes lesser for the smaller particle clusters (No. 30 and No. 40). Despite the reduced accuracy, a performance exceeding 50% implied that the tool correctly estimated a greater proportion of the evaluated sample than it misclassified, demonstrating its potential to estimate soil particle size.

A previous study investigated the use of the minor diameter of particles, assuming these particles have an ellipsoidal shape [14]. In this context, the minor diameter is appropriate because it aligns with the concept of percent passing, where the proportion of particles smaller than the sieve opening is compared to the total number of particles in the sample. However, in this study, the considerations made in classifying the particles for image analysis is through grouping them according to the sieve openings where each particle were retained. In practice, particles are retained on a specific sieve if at least one of their dimensions exceeds the sieve opening, which aligns with the concept being applied in identifying the maximum dimension as the representative particle size to validate the tool's capacity to estimate particle size. An illustration of this concept is presented in Figure 12, highlighting that the maximum dimension (Feret diameter) is the more suitable metric for the analysis of results in the current context. This approach is more aligned to the physical behavior of particles being retained in a sieve analysis.

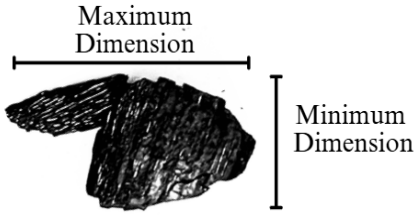

Fig. 12 Particle Size Dimension Considerations

The validation metrics indicate that the accuracy by area is consistently higher than the accuracy by number of particles in estimating particle size. Using the maximum Feret diameter, the program achieved an accuracy of 94.53% by area, compared to 83.89% by count, corresponding to 302 correctly classified particles out of 360. Conversely, when using the minimum Feret diameter, the accuracy dropped to 88.95% by area and 61.94% by count, with only 223 out of 360 particles correctly classified. In conjunction with other studies, an area-based validation is suggested in image analysis, as particle area has been shown to correlate more strongly with particle mass based of the density of these particles [14]. If the minimum dimension were used instead, there is a higher risk of falsely classifying particles into finer groups, since smaller dimensions do not reflect actual retention behavior. This is evidenced by the results gathered in the study, highlighting drastic differences in some groups, while some particle groups had only a slight decrease in the accuracy metric measured.

The recorded accuracy by area considering the maximum Feret diameter suggested the potential of the program to identify particle sizes through the concept employed. In this study, the particle sizes considered were particles classified as gravel or sand. To improve the capacity of the proposed technique, recalibration can be conducted to improve the pixel-to-mm scaling factor. Moreover, the camera settings may be adjusted, but this would require recalibration through the steps prescribed in the methodology. With these added refinements, the proposed approach shows relative ease with which the experimental setup can be replicated and improved, allowing continuous recalibration and refinement of the technique in future studies aimed at improving its accuracy and applicability.

5. CONCLUSION

Particle size was estimated using image processing. The developed program was able to identify particle sizes by making use of the bounding rectangle for each individual particle identified. The particle size for each particle is estimated accurately if the dimensions correspond to interval of the size between sieves where the particle was retained. Only individual particles were considered, since packed particles caused inaccurate measurements. The developed program achieved an accuracy of 94.53% by area and 83.89% by particle count using the maximum Feret diameter, whereas the minimum Feret diameter produced an 88.95% accuracy by area and 61.94% by count. These findings indicate that the maximum Feret diameter is a more appropriate metric for particle size estimation by sieve-based classification. The study also highlighted that while the program could estimate particle sizes as small as 0.13 mm (equivalent to one pixel), accuracy decreased for finer particle groups (e.g., No. 30 and No. 40). Overall, this methodology shows potential for wider applications in particle size estimation. Furthermore, the repeatability of the proposed acquisition setup facilitates a systematic recalibration and iterative refinement procedure, which supports future enhancements to the accuracy, reliability, and practical feasibility for use of the proposed technique.

The particle size estimates were limited to loosely packed particles, and as such, it is recommended to use higher-order image acquisition devices to assess the capacity of image processing techniques for estimating the size of clumped particles. In addition, studies may also incorporate the use of modal particle sizes in grid-based image analysis to create grain-size distribution curves for a larger image of soil. Further investigation into more refined calibration procedures is also recommended to enable reliable measurement of finer particles using image-based methods. Extending the proposed approach to three-dimensional analysis is another promising direction, as volumetric measurements may lead to more accurate comparisons with conventional sieve analysis results. Lastly, succeeding studies may investigate the extraction of particle shape descriptors and assess their potential use in supplementing the evaluation of soil mechanical properties.

6. ACKNOWLEDGMENTS

The researcher would like to thank the Department of Science and Technology Science Education Institute (DOST-SEI) for funding the study and the Department of Civil Engineering (DCE) of De La Salle University (DLSU) for their continuous guidance in his research work.

7. REFERENCES

[1] Joos L. and De Tender C., Soil under stress: The importance of soil life and how it is influenced by (micro)plastic pollution, Computational and Structural Biotechnology Journal, Vol. 20, 2022, pp. 1554-1566.

[2] Chen J., Wang E., Xue J., Cui L., Zheng X. and Du Q., Effects of soil particle size and gradation on the transformation between shallow phreatic water and soil water under laboratory freezing-thawing action, Journal of Hydrology, Vol. 619, 2023, pp. 1-13.

[3] Zhao J., Peng L., Hao Z., Wang J., Wang D. and Qi J., A novel large-scale direct shear apparatus considering size effects on strength of frozen coarse-grained soils, Transportation Geotechnics, Vol. 48, 2024, pp. 1 - 11.

[4] ASTM International, Standard Test Method for Particle-Size Distribution (Gradation) of Soils Using Sieve Analysis, 2017, https://www.astm.org/d6913-04r09e01.html.

[5] ASTM International, Standard Test Method for Particle-Size Distribution (Gradation) of Fine-Grained Soils Using the Sedimentation (Hydrometer) Analysis, 2021, https://www.astm.org/d7928-21e01.html.

[6] Dipova N. Determining the grain size distribution of granular soils using image analysis, Acta geotechnica slovenica, Vol. 14, Issue 1, 2017, pp. 29-37.

[7] Pattanawiwattanaporn W. and Thongkumsamut, C., Carbon balance attribution and storage in Khon Kaen University, Thailand. International Journal of GEOMATE, Vol. 29, Issue 134, 2025, pp. 184-192.

[8] Bherde V. and Balunaini U., Non-invasive based infrared thermography approach for field assessment of surface erosion in tailing dams. International Journal of GEOMATE, Vol. 29, Issue 132, 2025, pp. 150-157.

[9] Casita C.B., Iranata D., Suswanto B. and Matsumura M., Graphical representation of

uniaxial tensile test through digital image correlation. International Journal of GEOMATE, Vol. 27, Issue 122, 2024, pp. 28-35.

[10] Aryanto A., Revolis M., Oribe Y. and Yo H., Application of digital image correlation method in RC and FRC beams under bending test. International Journal of GEOMATE, Vol. 24, Issue 101, 2023, pp. 118-125.

[11] Igathinathane C., Pordesimo L. O., Columbus E. P., Batchelor W. D., and Methuku S. R., Shape identification and particles size distribution from basic shape parameters using ImageJ, Computers and Electronics in Agriculture, Vol. 63, Issue 2, 2008, pp. 168–182.

[12] Salawu E. Y., Elvi, A. O., Ajayi O. O., Ongbali S. O., and Afolalu S. A., Particle size distribution analysis of carburized HT250 gray cast iron using ImageJ, Materials Today: Proceedings, Vol. 105, 2024, pp. 227-239.

[13] Lim H., Cheon E., Lee D., Jeon J. and Lee S., Classification of Granite Soils and Prediction of Soil Water Content Using Hyperspectral Visible and Near-Infrared Imaging, Sensors, Vol. 20, Issue 6, 2020, pp. 1-15.

[14] Kumara J.J., Hayano K., & Kikuchi Y., Evaluation of area- and volume-based gradations of sand-crushed stone mixture by 2D images, KSCE Journal of Civil Engineering, Vol. 21, Issue 3, 2016, pp. 774-781.

[15] Pandiri D. N. K., Murugan R. and Goel T., Smart soil image classification system using lightweight convolutional neural network, Expert Systems with Applications, Vol. 238, 2024, pp. 1-18.

[16] Huang W., Miao H., Jiao S., Miao W., Xiao C., and Wang, Y., A planar constraint optimization method to improve camera calibration for imperfect planar targets, Optics and Lasers in Engineering, Vol. 180, 2024, pp. 1-9.

[17] Stankiewicz O., Lafruit G., and Domanski M., Multiview video: Acquisition, processing, compression, and virtual view rendering, Academic Press Library in Signal Processing, Vol. 6, 2018, pp. 3-74.

[18] Uy E.E.S. and Boonyatee T., Image Processing for Geotechnical Laboratory Measurements, International Journal of GEOMATE, Vol. 10, Issue 22, 2016, pp. 1964-1970.

[19] Uy E.E.S., Noda T., Nakai T. and Dungca J.R.D., Monitoring the Triggering of Liquefaction using Image Processing, International Journal of GEOMATE, Vol. 15, Issue 51, 2018, pp. 180-187.

[20] Uy E.E.S., Noda T., Nakai T. and Dungca J.R.D., Non-contact Estimation of Strain Parameter-triggering Liquefaction, International Journal of GEOMATE, Vol. 16, Issue 57, 2019, pp. 82-88.